Lawrence Berkeley National Laboratory
Recent Work

Title
Studies of the Role of Fault Zones on Fluid Flow Using the Site-Scale

Permalink
https://escholarship.org/uc/item/8697x4qv

Authors
Wittwer, C.S.
Chen, G.
Bodvarsson, G.S.

Publication Date
1993

eScholarship.org Powered by the California Digital Library
University of California

LBL-33565
UC-200

Lawrence Berkeley Laboratory
UNIVERSITY OF CALIFORNIA

EARTH SCIENCES DIVISION

Presented at the International High Level Radioactive
Waste Management Conference, Las Vegas, NV,
April 26–30, 1993, and to be published in the Proceedings

Studies of the Role of Fault Zones on Fluid Flow Using the Site-Scale Numerical Model of Yucca Mountain

C.S. Wittwer, G. Chen, and G.S. Bodvarsson

January 1993

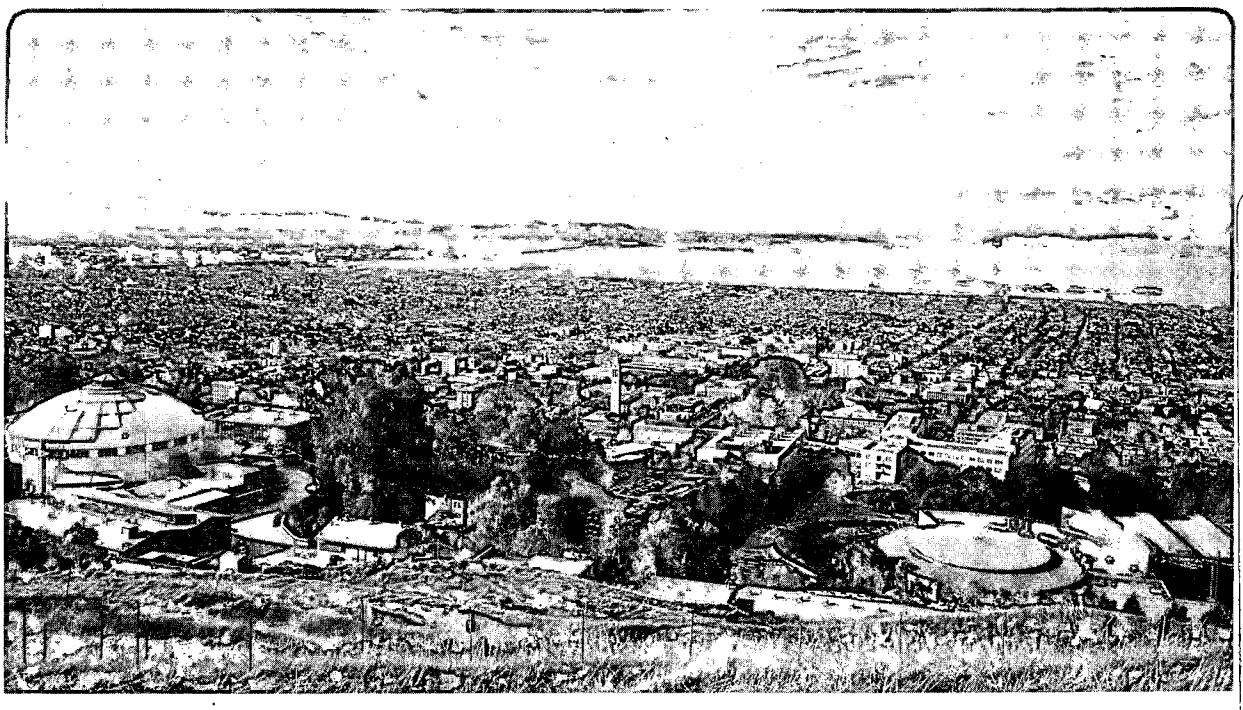

| REFERENCE COPY |
| Does Not |
| Circulate |
Copy 1
LBL-33565
Bldg. 50 Library.

Prepared for the U.S. Department of Energy under Contract Number DE-AC03-76SF00098

DISCLAIMER

This document was prepared as an account of work sponsored by the United States Government. Neither the United States Government nor any agency thereof, nor The Regents of the University of California, nor any of their employees, makes any warranty, express or implied, or assumes any legal liability or responsibility for the accuracy, completeness, or usefulness of any information, apparatus, product, or process disclosed, or represents that its use would not infringe privately owned rights. Reference herein to any specific commercial product, process, or service by its trade name, trademark, manufacturer, or otherwise, does not necessarily constitute or imply its endorsement, recommendation, or favoring by the United States Government or any agency thereof, or The Regents of the University of California. The views and opinions of authors expressed herein do not necessarily state or reflect those of the United States Government or any agency thereof or The Regents of the University of California and shall not be used for advertising or product endorsement purposes.

Lawrence Berkeley Laboratory is an equal opportunity employer.

This publication has been reproduced from the best available copy

DISCLAIMER

This document was prepared as an account of work sponsored by the United States Government. While this document is believed to contain correct information, neither the United States Government nor any agency thereof, nor the Regents of the University of California, nor any of their employees, makes any warranty, express or implied, or assumes any legal responsibility for the accuracy, completeness, or usefulness of any information, apparatus, product, or process disclosed, or represents that its use would not infringe privately owned rights. Reference herein to any specific commercial product, process, or service by its trade name, trademark, manufacturer, or otherwise, does not necessarily constitute or imply its endorsement, recommendation, or favoring by the United States Government or any agency thereof, or the Regents of the University of California. The views and opinions of authors expressed herein do not necessarily state or reflect those of the United States Government or any agency thereof or the Regents of the University of California.

LBL-33565

Studies of the Role of Fault Zones on Fluid Flow Using the Site-Scale Numerical Model of Yucca Mountain

C. S. Wittwer, G. Chen, and G. S. Bodvarsson

Earth Sciences Division
Lawrence Berkeley Laboratory
University of California
Berkeley, California 94720

January 1993

This work was carried out under U.S. Department of Energy Contracts DE-AC03-76SF00098 and DE-AI08-78ET44802, administered by the Nevada Operations Office, U.S. Department of Energy, in cooperation with the United States Geological Survey, Denver.

Printed on recycled paper

STUDIES OF THE ROLE OF FAULT ZONES ON FLUID FLOW USING THE SITE-SCALE NUMERICAL MODEL OF YUCCA MOUNTAIN.

C.S. Wittwer, G. Chen and G.S. Bodvarsson
Earth Sciences Division
Lawrence Berkeley Laboratory
One Cyclotron Road
Berkeley, CA 94720
(510) 486-4789

ABSTRACT

The three-dimensional grid of the site-scale model developed for the unsaturated zone at Yucca Mountain was used to perform two-dimensional simulations with the TOUGH2 computer program. The grid geometry consists of seventeen non-uniform layers which represent the lithological variations within the four main welded and non-welded hydrogeological units. The fault zones are explicitely modeled as porous medium using various asssumptions regarding their permeabilities and characteristic curves. Matrix flow is approximated using the van Genuchten model, and the equivalent continuum approximation is used to account for fracture flow in the welded units. Steady state simulations are performed with various uniform infiltration rates. The results are interpreted in terms of the effect of the fault characteristics on the moisture flow distribution, and on the location and formation of preferential pathways.

I. INTRODUCTION

Lawrence Berkeley Laboratory (LBL) in cooperation with the United States Geological Survey (USGS) has developed a three-dimensional site-scale numerical model of the unsaturated zone at Yucca Mountain, Nevada. The hydrogeology of the site is controlled by fluid flow through heterogenous, unsaturated, fractured and porous layers of volcanic tuffs in an arid environment. The site-scale model covers an area of about 30 km^2 around the potential repository area, and is bounded by major fault zones to the north (Yucca Wash fault), east (Solitario Canyon fault), and west (Bow Ridge fault). The numerical grid was designed to be able to account for the geological and hydrogeological mechanisms which have been described in the literature as being relevant to moisture flow at Yucca Mountain (see for example Scott and Bonk,[1] and Montazer and Wilson[2]). Additional data treatment reported in Wittwer et al. (1992)[3] led to the development of a highly non-uniform numerical grid which reproduces the complex geology of this fractured region, and explicitely includes the offset of the hydrogeological units due to three major fault zones.

Fluid flow in fault zones at Yucca Mountain have been previously studied using various assumptions, such as fractured medium,[4] seepage face,[5] or altered single porosity and broken-up double porosity medium.[6] Through this work, important mechanisms and results relative to moisture flow in unsaturated fractured tuffs have been found In the two-dimensional simulations conducted by Rulon et al. (1986),[4] an increase in the average flux through Topopah Spring hydrogeological unit, and a reduction of the lateral flow towards the fault zones occured if the saturated permeability of the zone is decreased from $5x10^{-11}$ to $5x10^{-14}$ m^2. Wang et al. (1986)[5] studied the effect of a fault zone modeled as a seepage face (open boundary exposed to atmospheric pressure, no capillary force and infinite saturated permeability). They showed that even if the liquid saturation increases on the western side of the fault due to the tilting of the formations, no water enters the fault zone. They also emphasize that, when both matrix and fracture flow is assumed, flow in the Topopah Spring unit occurs within the partially saturated rock matrix at steady state conditions. Tsang et al. (1993)[6] showed that if the fault zone is modeled as a high permeable single-porosity or double-porosity medium, and if the capillary suction of the zone has the same type of dependence between the saturated permeability and a capillary scaling parameter as the adjacent rocks, the fault zone has little effect in channeling or enhancing downward flow. The liquid saturation in the fault zone is lower than that in the neighboring rocks, but the overall saturation and capillary pressure distributions away from the fault zone are not influenced.

The purpose of this paper is to present results of steady-state simulations performed with a two-dimensional numerical grid representing the hydrogeology of the site. Recently measured moisture retention curves[12] for the rock matrix are used. Fracture flow within the welded units is allowed for high liquid saturations, and fault zones are modeled as a porous medium with either very low or very high saturated permeability compared to the adjacent rocks. The results are interpreted in terms of the influence of major fault zones on the occurence and intensity of vertical and lateral moisture flow, and on the existence of preferential pathways. All of these conditions may strongly affect the site suitability and the overall performance of the potential repository. Two-dimensional, cross-sectional submodels extracted from the three-dimensional numerical grid of the site-scale model, were used to illustrate the

complex geometry of the hydrogeological units and their sublayers, and the variability in rock properties. Measurements of capillary pressure versus saturation performed on rock samples of Yucca Mountain were interpreted using methods developed by Brooks and Corey (1966),[7] and van Genuchten (1980),[8] to predict the relationships between relative permeability and capillary pressure for the unsaturated rocks. The equivalent continuum approximation described in Klavetter and Peters (1986),[9] was used to integrate fracture flow to matrix flow for welded tuffs. The steady-state numerical simulations were carried out using the integral finite-difference computer code TOUGH2 (Transport Of Unsaturated Groundwater and Heat),[10] and the moisture-flow distribution was calculated for various constant infiltration rates at the surface under the assumption that the fault zones behave as a porous medium with either high or low permeabilities. This work is in progress as there are many studies planed using the three-dimensional site-scale model.

II. THREE-DIMENSIONAL NUMERICAL GRID

The lithological section between the ground surface and the water table in the site-scale model area is represented by a series of massive and fractured welded parts of ashflow tuffs (Tiva Canyon-, Topopah Spring tuffs), and porous non-welded part of ashflow and ashfall tuffs (Yucca Mountain-, Pah Canyon-, Calico Hills-, Prow Pass-, Bullfrog tuffs, bedded tuffs). Due to their mechanical properties, these rocks have been characterized in the literature as hydrogeological units with different flow properties.[2] The spatial distribution of these units was defined in Wittwer et al. (1992)[3] by using available information on lithological logs from wells and surface data, and this information was used to design the numerical grid of the three-dimensional site-scale model.

The numerical grid consists of about 5000 elements and 20,000 connections. This grid was constructed by placing the center nodes for about 300 gridblocks at the location of existing and proposed boreholes, along the traces of major fault zones, or by distributing them in order to consider different infiltration zones, such as alluvium, sideslopes, ridgetops, as well as the spatial distributions of various types of outcrops, such as welded and non-welded tuffs. The horizontal grid for the site-scale model is shown in Fig. 1, and illustrates how the shapes of the gridblocks were created by a mesh-generator using the center nodal locations. At each of these center nodes, the four main hydrogeological units were vertically subdivided into about seventeen sublayers. These seventeen layers of gridblocks represent, as closely as possible, lithological variations within the main units; these include extremely massive vitrophyre layers at the border of the main ashflows, the occurence of lithophysae cavities within the welded units, and the presence of zeolitic alteration. The offsets along three fault zones, the Ghost Dance-, Abandoned Wash-, and Dune Wash faults, were explicitely represented within the three-dimensional grid by horizontally connecting the sublayers on each side of the faults through a double number of gridblocks. A mesh generator was used to create the connections, the volumes and the common surface areas of each gridblocks. The approach used, therefore, allows for the faults to be

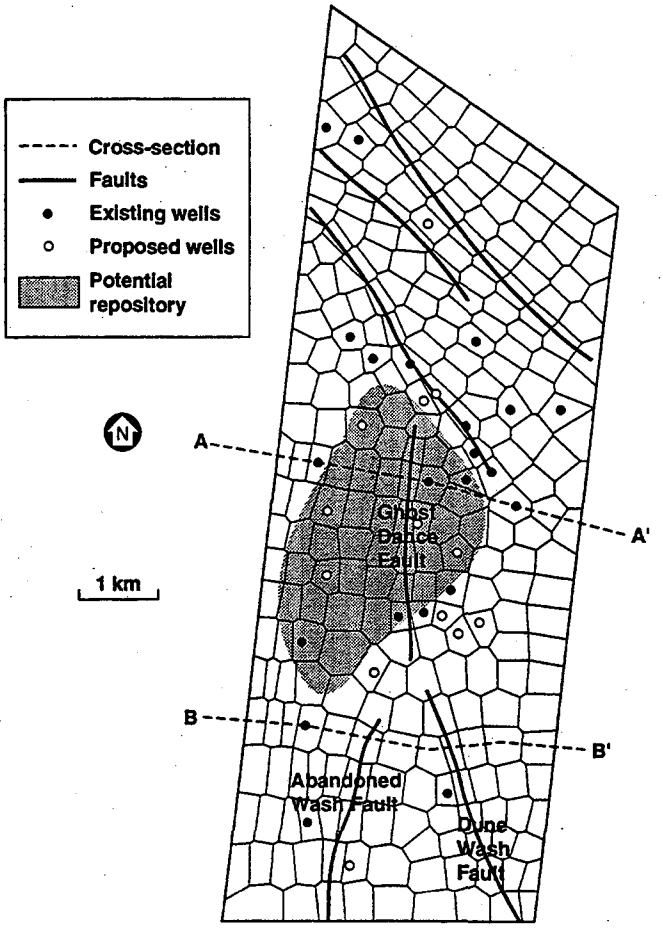

Fig.1: Horizontal grid for the site-scale model.

modeled explicitly, and the model geometry is consistent with the complex geology of this heavily faulted region. The computer developed grid also allows one to readily modify and adapt the non-uniform numerical grid to new data or new problems.

III. METHODOLOGY

Numerical simulations using two NW to SE two-dimensional cross-sections were performed with the computer code TOUGH2[10] which is based on the integral finite difference method, and accounts for the transport of moisture, air and heat in unsaturated porous and fractured media. In order to be able to compare the moisture distribution within blocks of rocks bounded by one and two fault zones, the location of the profiles was chosen so that the northern cross-section (A-A') cuts the site-scale model area at the level of the potential repository, and includes Ghost Dance fault (Fig.1). The second cross-section (B-B') is located about 3 km further to the south, and intersects the Abandoned Wash- and Dune Wash faults.

A. Rock matrix properties:

Representative values for the parameters of the rock matrix, such as rock density, porosity, absolute permeability were compiled from data found in the

literature.[11,12,13] for each of the seventeen model layers. Table 1 shows which rock types were assigned to the different layers, and the relevant hydrological data used for each layer. It should be noted that the available data are scarce so that the values given in Table 1 can only be considered as best current estimates, and will be subject to changes as the site-characterization studies proceed. The values used in the models were chosen based upon the distribution of the measured parameter values, the locations of the samples within the different units, and the lithological similarities within each of the hydrogeological layers.

Table1: Rock matrix properties for the seventeen model layers.

HYDRO-GEOLOGICAL UNIT	LITHOLOGY	SUB-LAYER	POROSITY RANGE (%)	POROSITY MODEL (%)	PERMEABILITY RANGE (m^2)	PERMEABILITY MODEL (m^2)	$\alpha \times 10^{-6}$ (Pa)	n	m
Tiva Canyon welded tuff	caprock upper cliff	1.1	6 - 24	17	2E-19 - 2E-14	1E-18	0.067	1.33	0.250
	upper lithophysae clinkstone zone lower lithophysae hackly zone columnar zone	1.2	6 - 28	17	1E-20 - 2E-16	2E-18	0.067	1.33	0.250
	vitrophyre	1.3	2 - 10	6	4E-17 - 1E-15	1E-18	0.067	1.33	0.250
Paintbrush non-welded tuff	shardy base	2.1	12 - 54	33	1E-17 - 5E-13	1E-13	1.67	1.20	0.167
	non-welded tuffs bedded tuffs	2.2	18 - 57	37	5E-16 - 5E-12	5E-14	6.00	1.19	0.163
	non-welded tuffs	2.3	10 - 55	32	4E-16 - 6E-13	1E-13	4.33	1.17	0.142
Topopah Spring welded tuff	vitrophyre	3.1	3 - 9	6		1E-18	0.067	1.41	0.290
	caprock rounded zone	3.2	9 - 22	15	8E-17 - 4E-14	4E-16	0.125	1.22	0.180
	upper lithophysae	3.3	10 - 16	13	5E-20 - 3E-18	4E-18	0.20	1.28	0.220
	middle non-lithophysae lower lithophysae	3.4	6 - 22	14	4E-20 - 1E-17	5E-18	0.133	1.33	0.250
	lower non-lithophysae	3.5	6 - 18	12	4E-20 - 1E-17	5E-18	0.067	1.33	0.250
	vitrophyre	3.6	1 - 10	5	5E-20 - 2E-17	1E-18	0.067	1.41	0.290
Calico Hills non-welded tuff	bedded tuffs	5.1	23 - 48	35		2E-13	2.0	1.15	0.130
	non-welded vitric bedded tuffs	5.2	8 - 48	28	1E-18 - 2E-15	3E-13	2.0	1.14	0.120
	non-welded tuffs	5.3	30 - 48	39		3E-13	2.0	1.14	0.120
	slightly zeolitized zeolitized, partly argillic zeolitized, devitrified zeolitized	5.4 5.5	14 - 36	25	5E-19 - 7E-17	1E-16	0.1	1.23	0.190

The van Genuchten model[8] was used in the simulations to account for the relationships between the effective saturation S_e, and the capillary pressure P_{cap} or relative permeability K_{rel} of the rock matrix.

$$S_e = \left[1 + (\alpha \cdot P_{cap})^n\right]^{-m}$$

where:

$$S_e = \frac{S_l - S_r}{S_s - S_r}$$

with : S_l = liquid saturation
S_r = residual saturation
S_s = satiated saturation

P_{cap} = capillary pressure
α, n, m = empirical fitting parameters

New moisture retention measurements performed on core and surface samples by Flint and Flint (1992)[14] were used in this study as these represent the best current available data set. Fitting parameters obtained with the Brooks and Corey model[7] for these measured curves, were employed to obtain the three empirical parameters of the van Genuchten model by applying equations given in Wang (1992).[15] The van Genuchten parameters shown in Table 1 for the seventeen layers in the model were chosen from the entire data set in order to represent the characteristic curves of each rock types. Values for layers which have not been explicitely measured were taken from rock samples with similar lithologies. The capillary pressure curves calculated with the van Genuchten model are given in Fig. 2a for the non-welded units, and in Fig. 2b for the welded units.

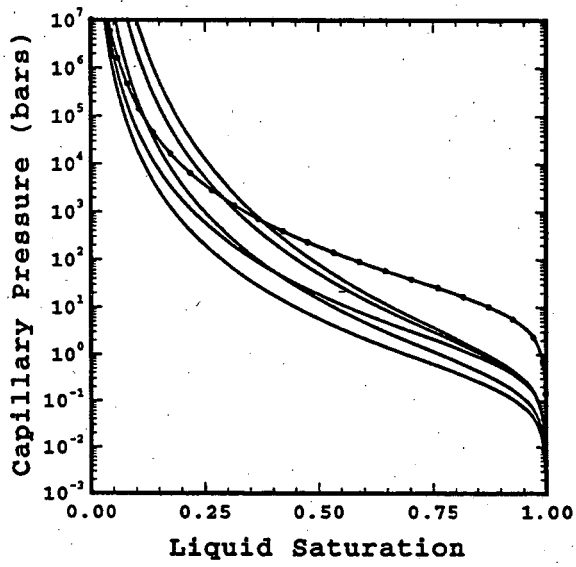

Fig.2a: Capillary pressure curves for the rock matrix of non-welded tuffs (Paintbrush-, and Calico Hills units).
Caption: the zeolitized tuffs are represented by a dotted line.

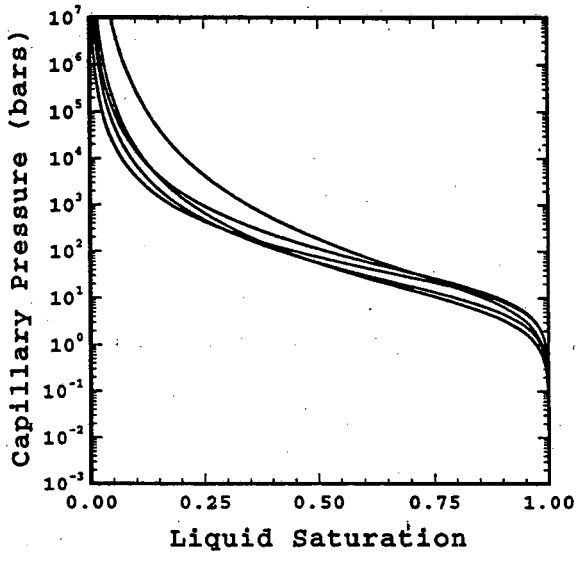

Fig.2b: Capillary pressure curves for the rock matrix of welded tuffs (Tiva Canyon-, and Topopah Spring units).

The van Genuchten model was also used to calculate the relative permeability curves for the rock matrix. The relationship between relative permeability k_{rel}, and effective saturation is given by:

$$k_{rel} = \sqrt{S_e}\left\{\left[1-(S_e)^{\frac{1}{m}}\right]^{\frac{1}{m}}\right\}^2$$

where:
S_e = effective saturation (see above)
m = fitting parameter (same as above)

B. Fracture properties

As a high fracture density has been reported in the literature for the welded units,[2] fracture flow representation was added to the rock matrix characteristic curves for Tiva Canyon- and Topopah Spring hydrogeological units. The equivalent continuum approximation developed by Klavetter and Peters (1986)[9] based on capillary equilibrium between matrix and fracture, was applied to calculate the threshold saturation S_{th} described in Pruess et al. (1990)[16] at which fracture flow begins:

$$S_{th} = \frac{\phi_m}{\phi_m + \phi_f}$$

where:
ϕ_f = fracture porosity (assumed equal to 0.001)
ϕ_m = matrix porosity

The approach used in the simulations assumes that the capillary pressure of the equivalent continuum is equal to that of the matrix until the threshold saturation, and that fracture flow, described here by a linear relationship between capillary pressure and saturation, dominates above the threshold saturation. Threshold saturations between 0.980 and 0.994 were obtained for the nine layers representing the welded Tiva Canyon and Topopah Spring units. As no capillary functions have been reported in the literature for fracture flow, the approach used in the simulations is based on the assumption that the fractured medium has the same pore size distribution as the rock matrix for each rock type. The absolute fracture permeability was taken to be equal to 10^{-11} m^2 based on values reported by Klavetter and Peters (1986).[9] The air entry value is predicted from the saturated permeability value k_s by using the scaling relationship proposed in Wang (1992):[15]

$$k_s = 2\frac{\sigma \cdot \cos(\theta) \cdot \alpha}{\rho \cdot g}$$

where:
σ = surface tension = 0.07183 $kg.s^{-2}$
θ = contact angle = 0°
α = capillary scaling factor = 1/air entry value, Pa^{-1}
ρ = water density = 1000 kg m^{-3}
g = gravitational acceleration = 9.8 m s^{-2}

The relative permeabilities were also scaled following the equivalent continuum approximation assuming that matrix and fracture flow obey the same function, and that their relative effect can be added above the threshold saturation value. The combined fracture and matrix characteristic curves are shown in Fig. 3 for the layers of the welded Tiva Canyon-, and Topopah Spring units. These curves show that fracture dominated flow begins between 1000 and 3500 Pa for the various sublayers. The approach used therefore assumes only matrix flow until very high liquid saturations are reached.

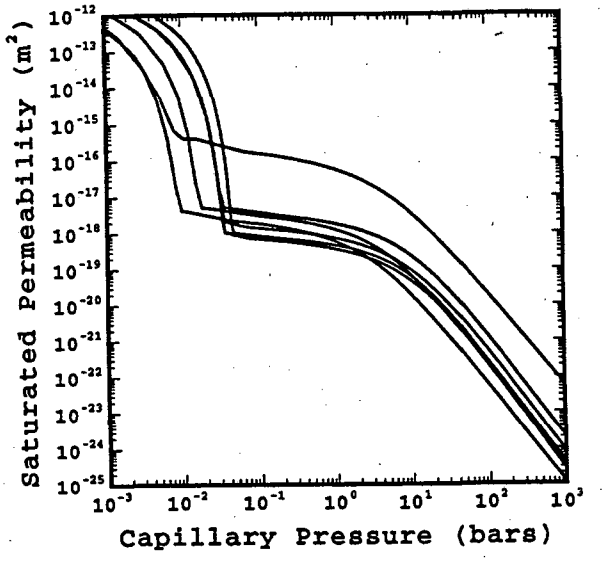

Fig. 3: Combined fracture and matrix characteristic curves for the welded tuffs of Tiva Canyon-, and Topopah Spring units.

C. Fault zone properties

The three fault zones are represented in the numerical grid by columns of gridblocks of about 200 to 350 m width. This large width is somewhat consistent with new field data about the lateral extent of the Ghost Dance Fault reported by Spengler et al. (1993).[17] In the present study, fault zones were treated as porous medium with either very high or very low permeability in comparison with the neighboring rock matrix. The van Genuchten model was used to calculate the capillary pressure curves shown in Fig. 4, as well as the relative permeability curves of the fault zones for these two different test cases. The scaling parameter α was calculated based on the assumed minimum and maximum saturated permeability (10^{-20} m^2 and 10^{-11} m^2 respectively) of the fault zones. The other fitting parameters m and n were chosen assuming that the pore size distribution of the fault zones is rather narrow (n = 2, m = 0.5 for high permeability fault, and n = 5 , m = 0.8 for low permeability fault). We have found that larger values of n for the fault zones give near-identical results but are more computationally intensive.

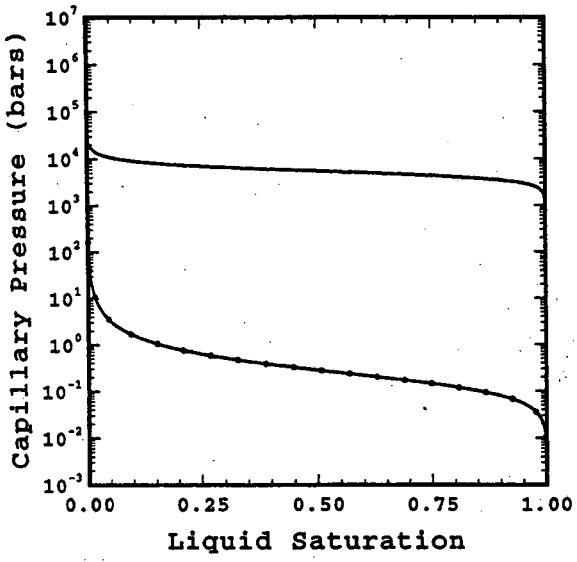

Fig. 4: Capillary pressure curves for the two fault zones.
Caption: the low permeability fault is represented by a continuous line, and the high permeability fault by a dotted line.

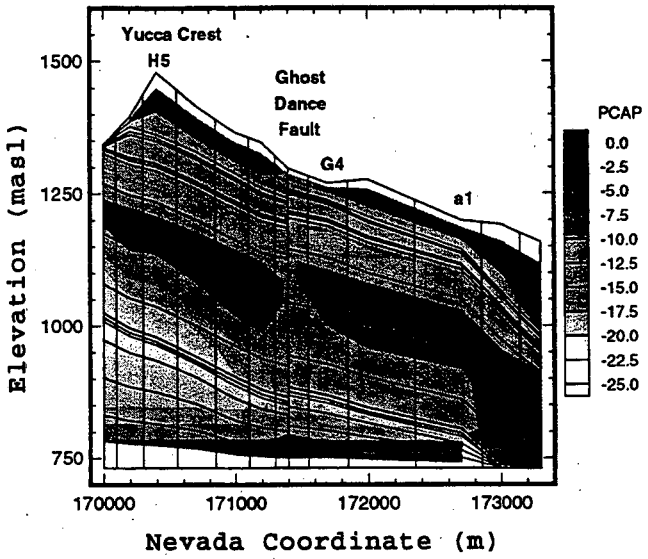

Fig.5a: Capillary pressure distribution for cross-section A-A' with infiltration rate of 10^{-1} mm y^{-1}, and a saturated permeability of 10^{-11} m^2 for the Ghost Dance fault.

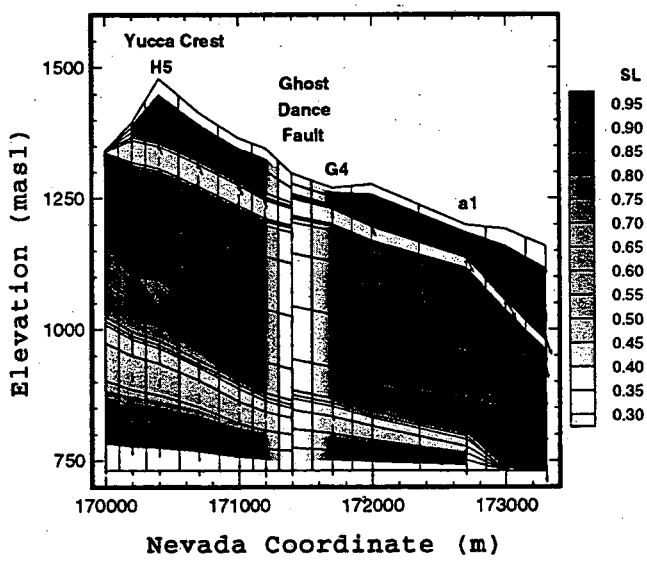

Fig.5b: Liquid saturation distribution for cross-section A-A' with infiltration rate of 10^{-1} mm y^{-1}, and a saturated permeability of 10^{-11} m^2 for the Ghost Dance fault.

IV. RESULTS OF TWO-DIMENSIONAL NUMERICAL SIMULATIONS

Capillary and saturation distributions for the two-dimensional vertical cross-sections were calculated using the TOUGH2 simulator for three spatially uniform infiltration rates of 10^{-1} to 10^{-3} mm y^{-1}.

A. High permeability fault zone

Results for the set of simulations using the maximum infiltration rate of 10^{-1} mm y^{-1} used in this study, are shown in Fig. 5a for capillary pressure, and in Fig. 5b for liquid saturation. The capillary pressure values are consistently above -10 bars in all layers, except near the western boundary where a low capillary pressure zone (-22 bars) occurs near the top layers of Calico Hills. This low capillary pressure zone is probably due to decreased vertical flow due to increased lateral flow in the upper layers of the Topopah Spring unit. The capillary pressure still decreases in the Tiva Canyon unit, down to the middle of Topopah, where the pressure reaches -2 bars due to the high saturation of a low permeable layer (layer representing the upper lithophysae zone). As it can be seen on Fig. 5b, the low liquid saturation (0.03) in the fault zones is a predominant feature of these simulations, and is due to the characteristic curves that were chosen. High liquid saturations are found in Tiva Canyon (0.97-0.91), Paintbrush (0.78-0.93), and Topopah Spring (0.65-0.90).

The saturation distribution shows three distinct features. Firstly, the liquid saturation in the Tiva Canyon unit decreases with depth. A high saturation zone (0.98) occurs at the bottom of Topopah Spring just above the water table in the eastern part of the model, and propagates westward at the contact with the Calico Hills vitric layers slightly further than the Ghost Dance fault.

Another set of simulations were performed with a decreased infiltration rate of 10^{-2} mm y^{-1}. In this case, the capillary pressure increases uniformly from about -20 bars near the ground surface to zero at the water table, except near the western boundary where the low capillary pressure zone of -28 bars is found in the lower part of the Topopah Spring unit. The capillary pressure in the fault zone is again uniform, but has increased to -10 bars. The saturation distribution is similar to the previous simulations, but the liquid saturations have decreased to 0.84-0.80 in Tiva Canyon, to 0.40-0.53 in Paintbrush, and to 0.65-0.90 in Topopah Spring.

Numerical simulations were also run to reach steady state with an infiltration rate of 10^{-3} mm yr $^{-1}$. The capillary pressure distribution obtained for this very low rate does not deviate strongly from static conditions, but the capillary pressure near the ground surface is decreased from -70 and -50 bars depending on the elevation to -40 and -30 bars, respectively. The capillary pressure in the fault zone stays uniformly around -17 bars, and increases close to the water table. The liquid saturations S_l of different units vary within well defined limits, such as Tiva Canyon: 0.77-0.67, Paintbrush: 0.35-0.45, Topopah Spring: 0.60-0.85, Calico Hills vitric: 0.55-0.70, and Calico Hills zeolitic: 0.90-0.99.

B. Low permeability fault zone

Except within the Ghost Dance fault zone, the overall capillary pressure and liquid saturation distributions are similar to those obtained for the high permeability fault. In the case of 10^{-1} mm y^{-1} infiltration rate, the main difference is that the capillary pressure in the middle of Topopah Spring unit reaches -2 bars, and even -1 bars in the fault zone at the same elevation. However, in this case very high liquid saturations are found in the fault zone because of the assumed characteristic curves.

C. Effect of two fault zones (simulations with cross-section B-B')

In this cross-section two fault zones (the Abandoned Wash fault and the Dune Wash fault) are intersected as is clearly seen in the capillary pressure and saturation distributions. Except for a few details, the distribution using high and low permeability fault zones do not differ significantly from the equivalent cases including only the Ghost Dance fault. The main difference concerns the location and the intensity of the low capillary pressure zone located at the boundary between Topopah Spring and Calico Hills units. The results for the simulations with 10^{-2} mm y^{-1} infiltration rate shown in Fig. 6a for capillary pressure, and Fig. 6b for liquid saturation, show that the location of this low capillary pressure zone (-36 bars) is now centered at the top of Calico Hills. A similar capillary pressure zone (-20 bars) occurs in the block between the two faults, but in the lower part of Topopah Spring. For 10^{-1} mm y^{-1} infiltration rate, the low capillary pressure zone (-25 bars), again centered near the top of Calico Hills, has moved eastward to the third gridblock, just below Yucca Mountain crest. The liquid saturation distribution presented in Fig. 6b illustrates the dominant influence of the fault zones, and the high saturations of all units, except the Paintbrush unit.

D. Vertical and lateral flow

The occurence and intensity of lateral flow was studied by normalizing the vertical moisture flow between layers by the constant assumed infiltration rate at the ground surface (normalized flow = V). Lateral flow occurs when the vertical flow is diverted because of the tilting of the layers, and may be enhanced by the permeability contrast. In our simulations, this lateral eastward flow is terminated by the fault zones, because of their assumed flow characteristics. The dependence of the lateral flow intensity on the degree of tilting can be seen in our simulations because the cross-sections include several blocks with increasing slopes. Whereas vertical flow is dominant in most of the simulations, increased lateral flow appears in the upper part of Topopah above the upper

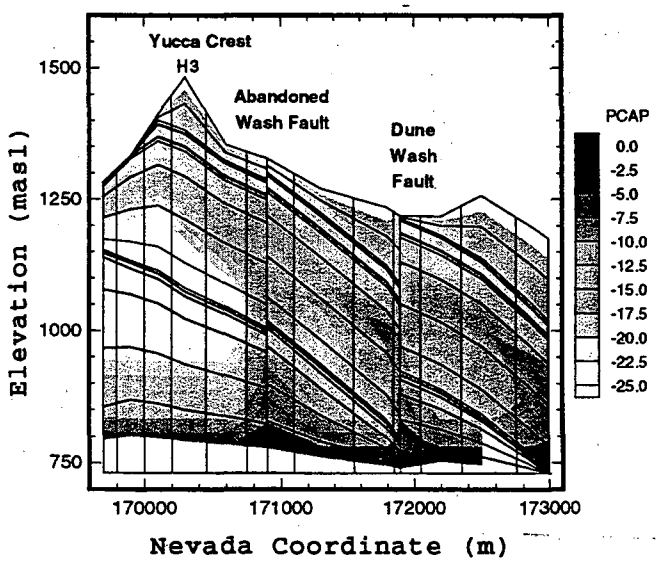

Fig.6a: Capillary pressure distribution for cross-section B-B' with infiltration rate of 10^{-2} mm y^{-1}, and a saturated permeability of 10^{-20} m^2 for the Abandoned Wash-, and Dune Wash faults.

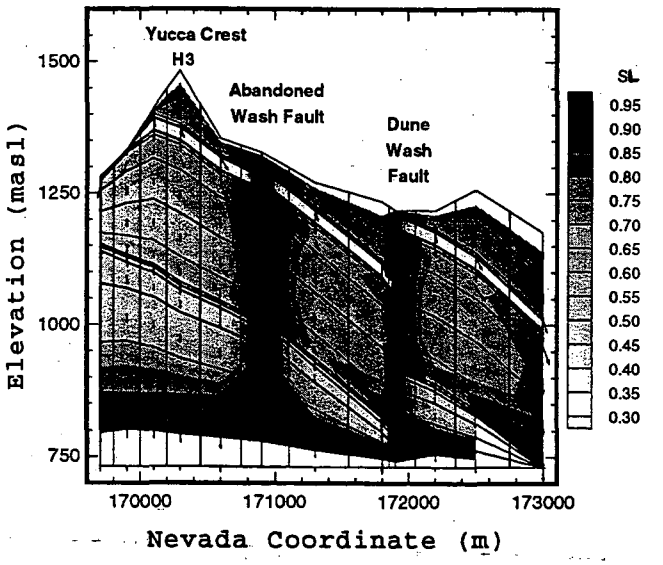

Fig.6b: Liquid saturation distribution for cross-section B-B' with infiltration rate of 10^{-2} mm y^{-1}, and a saturated permeability of 10^{-20} m^2 for the Abandoned Wash-, and Dune Wash faults.

lithophysae zone (layer representing the rounded zone). As the intensity of lateral flow depends on the length of the flow path, and the volume of the drainage zone, the flows calculated on the eastern side of the Abandoned Wash-, and Dune Wash faults are smaller than those defined at the Ghost Dance fault.

Vertical flow rates were also studied within the Ghost Dance fault zone. The vertical normalized flow rate V through the high permeable fault zone varies from about 1.0 near the ground surface for high infiltration rates to very small values above the water table for low infiltration rates . A general feature shows a strong decrease in vertical flow rate V with depth in the fault zone, suggesting that water flows into the adjacent formation. This phenomenon mainly happens for lower infiltration rates (V down to 0.05), and is reduced (V=0.9) at higher infiltration rate (I= 10^{-1} mm y^{-1}). This effect seems to be limited to the gridblocks close to the fault zone. Our results suggest that this lateral flow out of the fault zone may happen not only in the Paintbrush and top of Topopah Spring unit, but also between the middle part of Topopah and the water table. The reason for this outflow from the fault zone is again the characteristic curves used. High flow within the fault zone results in relatively high capillary pressures, hence the moisture evades the fault zone for the lower (more negative) capillary pressure surrounding rocks.

The vertical flow through Topopah Spring unit varies from about 0.6 to 1.6 times the infiltration rate between Solitario Canyon fault at the western boundary of the cross sections, and the Ghost Dance fault.

Outside of the fault zones, the main moisture flux is vertically transmitted through the layers, and the lateral flow remains about 100 times lower than the vertical one, and even lower in the very low permeability vitrophyre layers. Strong eastward lateral flow mainly occurs in the top of Topopah, in the more permeable layer representing the rounded zone. Weaker lateral flow also occurs in the first layer of the Paintbrush unit, just below the very low permeable vitrophyre layer of Tiva Canyon. Small westward lateral flow is created on the east side of Yucca Mountain for cross-section B-B' perhaps due to grid effects.

The various simulations show that perched water zones do not occur in the present set of simulations, because of the relatively low infiltration rates used. Potential zones are located in the base of Topopah Spring, especially east of Ghost Dance fault. Future work will include higher infiltration rates and different representations of the fault zones.

V. CONCLUSION

Two-dimensional simulations were carried out to investigate the role of major faults (Ghost Dance-, Abandoned Wash-, and Dune Wash faults) on fluid flow within the unsaturated zone of the site-scale model. As hydrological properties of these faults are not known at present, bounding calculations were performed in order to study the effect of the faults. The faults were assumed to be either very high permeable and have a low potential capillary pressure, or very low permeable and possess large potential capillary pressure. The approach taken in the design of the numerical grid, and the numerical capabilities of the TOUGH2 simulator allows one to analyze the results in terms of preferential pathways, lateral flow, and capillary barriers.

All results shown here are strongly dependent on the characteristic curves chosen for the different rock types. The different hydrogeological units, and their main lithological variations were modeled as porous layers by including various matrix rock properties, such as porosity, absolute permeability, relative permeability and capillary pressure curves, for the seventeen layers of the model. The massive welded fractured tuffs were modeled by using the equivalent continuum approximation for matrix and fracture flow.[9] Properties for the fault zones were chosen to represent two extreme conditions, such as a porous permeable or impermeable zone. The distribution of moisture-flow was calculated for infiltration rates varying over three orders of magnitude.

In the case of a permeable fault, the assumed characteristic curves result in relatively high capillary pressures and very low liquid saturations at steady state. This in turn prevents flow from neighboring formations to enter the fault, and in fact some of the infiltration prescribed on the top of the fault is lost to those surrounding rocks. One would only get significant vertical flow in a fault if its properties are such that the characteristic curves are similar to those of the adjacent formations (e.g. not much lower air entry value), and the absolute saturated permeability is significantly larger.

ACKNOWLEDGMENT

This work was prepared under U.S. Department of Energy contract no. DE-AC03-76SF00098, and DE-A108-78ET44802 administered by the Nevada Operations Office in cooperation with the U.S. Geological Survey, Denver. Review of this paper by Y. Tsang and T. Hadgu, LBL, is greatly appreciated. The authors also appreciate the contributions of M. Chornack, A. Flint, L. Flint, E. Kwiclis, and R. Spengler, U. S. Geological Survey, to this work.

REFERENCES

1. R.B. SCOTT and J. BONK, "Preliminary Geologic Map of Yucca Mountain with Geologic Sections, Nye County, Nevada", Open-File Report 84-494, U.S. Geological Survey , scale 1:12,000 (1984).

2. P. MONTAZER and W.E. WILSON, "Conceptual Hydrologic Model of Flow in the Unsaturated Zone, Yucca Mountain, Nevada," Water Resources Investigations Report 84-4355, U.S. Geological Survey (1984).

3. C.S.WITTWER, G.S. BODVARSSON, M.P. CHORNACK, A.L. FLINT, L.E. FLINT, B.D. LEWIS, R.W. SPENGLER, and C.A. RAUTMAN, "Design of a three-dimensional site-scale model for the unsaturated zone at Yucca Mountain, Nevada," Proceedings of the Third International High Level Radioactive Waste Management Conference, Las Vegas, 263-271 (1992).

4. J. RULON, G.S. BODVARSSON, and P. MONTAZER, "Preliminary simulations of groundwater flow in the unsaturated zone, Yucca Mountain, Nevada," LBL-20553, Lawrence Berkeley Laboratory (1986).

5. J.S.Y. WANG and T.N. NARASIMHAN, "Hydrologic modeling of vertical and lateral movement of partially saturated fluid flow near a fault zone at Yucca Mountain," LBL-23510, Lawrence Berkeley Laboratory, and SAND87-7070, Sandia National Laboratories (1988).

6. Y.W. TSANG, K. PRUESS, and J.S.Y. WANG, "The role of fault zone in affecting multiphase flow at Yucca Mountain," This issue.

7. R.H. BROOKS and A.T. COREY, " Properties of porous media affecting fluid flow," J. Irrigation and Drainage Div., Proc. Am. Soc. Civ. Eng., 92, IR2, 61-88 (1966)

8. M.Th. VAN GENUCHTEN, " A Closed-Form Equation for Predicting the Hydraulic Conductivity of Unsaturated Soils," Soil. Sci. Soc. Am. J., 44, 892-898 (1980).

9. E.A. KLAVETTER and R.R. PETERS, "Estimation of hydrologic properties of an unsaturated fractured rock mass," SAND84-2642, Sandia National Laboratories (1986).

10. K. PRUESS, "TOUGH2-A General-purpose Numerical Simulator for Multiphase Fluid and Heat Flow," LBL-29400, Lawrence Berkeley Laboratory (1990).

11. L.E. FLINT and A.L. FLINT, "Preliminary Permeability and Water-retention Data for Nonwelded and Bedded Tuff Samples, Yucca Mountain Area, Nye county, Nevada," Open-File Report 90-569, U.S. Geological Survey (1990).

12. L.E. FLINT and A.L. FLINT, "Porosity, and permeability data for surface and well samples at Yucca Mountain," Oral communication, U.S. Geological Survey (1992).

13. P.H. NELSON, D.C. MULLER, U. SCHMISCHAL, and J.E. KIBLER, "Geophysical logs and core measurements from forty boreholes at Yucca Mountain, Nevada," Geophysical Investigations Map MAP GP-1001, U.S. Geological Survey (1991).

14. L.E. FLINT and A.L. FLINT, "Rock matrix property data for a schematic cross-section at well UZ16, Yucca Mountain," Oral communication, U.S. Geological Survey (1992)

15. J.S.Y. WANG, "Variations of hydrological parameters of tuff and soil," Proceedings of the Third International Conference on High-Level Radioactive Waste Management, Las Vegas, 727-731 (1992).

16. K. PRUESS, J.S.Y. WANG, and Y.W. TSANG, "On thermohydrological conditions near high-level nuclear wastes emplaced in partially saturated fractured tuff, Part 2. Effective continuum approximation," Water Resour. Res., 26(6), 1249-1261 (1990).

17. R.W. SPENGLER, C.A. BRAUN, R.M. LINDEN, L.G. MARTIN, D.M. ROSS-BROWN, and R.L. BLACKBURN, " Structural character of the Ghost Dance Fault, Yucca Mountain, Nevada," This issue.

LAWRENCE BERKELEY LABORATORY
UNIVERSITY OF CALIFORNIA
TECHNICAL INFORMATION DEPARTMENT
BERKELEY, CALIFORNIA 94720